## General Disclaimer

## One or more of the Following Statements may affect this Document

- This document has been reproduced from the best copy furnished by the organizational source. It is being released in the interest of making available as much information as possible.

- This document may contain data, which exceeds the sheet parameters. It was furnished in this condition by the organizational source and is the best copy available.

- This document may contain tone-on-tone or color graphs, charts and/or pictures, which have been reproduced in black and white.

- This document is paginated as submitted by the original source.

- Portions of this document are not fully legible due to the historical nature of some of the material. However, it is the best reproduction available from the original submission.

# TECHNICAL REPORT

## AN INVESTIGATION OF S-BAND SIGNAL TRANSMISSION THROUGH AN APOLLO EARTH-ENTRY PLASMA

By: Donald W. Boyer

## CAL No. AI-2187-A-11

Prepared For:

National Aeronautics and Space Administration
Goddard Space Flight Center
Greenbelt, Maryland 20771

TECHNICAL REPORT
Contract No. NAS5-9978
June 1969



CORNELL AERONAUTICAL LABORATORY, INC.
OF CORNELL UNIVERSITY, BUFFALO, N. Y. 14221

07

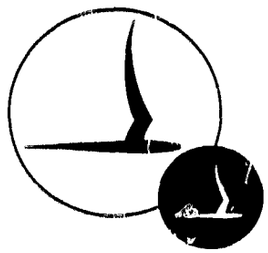

CORNELL AERONAUTICAL LABORATORY, INC.
BUFFALO, NEW YORK 14221

# AN INVESTIGATION OF S-BAND SIGNAL TRANSMISSION THROUGH AN APOLLO EARTH-ENTRY PLASMA

CAL NO. AI-2187-A-11
CONTRACT NO. NAS5-9978
JUNE 1969

Prepared For:

NATIONAL AERONAUTICS AND SPACE ADMINISTRATION
GODDARD SPACE FLIGHT CENTER
GREENBELT, MARYLAND 20771

PREPARED BY: Donald W. Boyer
*Donald W. Boyer*

APPROVED BY: Charles E. Treanor
*Charles E. Treanor, Head*
*Aerodynamic Research Department*

## FOREWORD

This investigation was supported by the National Aeronautics and Space Administration, Goddard Space Flight Center, Greenbelt, Maryland, under Contract NAS5-9978.

TABLE OF CONTENTS

## ABSTRACT

An investigation has been made of signal transmission at S-band through an Apollo earth-entry plasma environment. A plasma profile has been described which is consistent with numerical predictions of the Apollo flow field and which results in computed signal attenuation behavior in qualitative agreement with data recorded from the AS-501 fired entry flight of an Apollo Command Module. The study has indicated that plane-wave considerations alone are inadequate and that antenna impedance variation effects must be included to afford a quantitative correlation with observed attenuation behavior. The considerations have included the effect of a dielectric aperture window on the calculated far-field transmission loss as well as an indication of the effect of radiation propagation angle on the shape of the received S-band signal.

# NOMENCLATURE

| | |
|---|---|
| $a$ | Half-width of rectangular waveguide |
| $d$ | Thickness of separated flow region |
| $\ell$ | Plasma thickness |
| $n_e$ | Electron number density |
| $t$ | Dielectric window thickness |
| $\|T\|^2$ | Far-field transmission loss |
| $\|T_{FS}\|^2$ | Plane-wave transmission loss (plasma bounded by free space) |
| $\|T_{GP}\|^2$ | Plane-wave transmission loss (plasma adjacent to a ground plane) |
| $Y$ | Complex antenna admittance |
| $\alpha$ | Attenuation constant |
| $\Gamma$ | Complex voltage reflection coefficient |
| $\varepsilon'/\varepsilon_o$ | Relative dielectric constant |
| $\varepsilon''/\varepsilon'$ | Loss tangent |
| $\eta$ | Plasma refractive index |
| $\lambda$ | Radiation wavelength |
| $\nu_c$ | Electron collision frequency |
| $\omega$ | Radian signal frequency |

Subscripts

| | |
|---|---|
| o | Value in free space |
| p | Value in plasma |
| G, guide | Value in waveguide |
| diel | Value in dielectric |

# I. INTRODUCTION

The present note on S-band signal transmission through an Apollo earth entry plasma represents a brief adjunct to a comprehensive program of research which has been continuing at CAL over the past several years on an investigation of the Apollo earth-entry communications blackout problem.[1]

In broad scope, this latter program has been concerned, theoretically, with obtaining a complete solution for the asymmetric flow field about the Apollo vehicle at angle of attack, and experimentally, with the measurement of the rate coefficients of the important electron removal mechanisms in the plasma enveloping the Apollo vehicle at superorbital entry velocities. These data are then employed in the computation of the flow field electron number density and collision frequency profiles for the ultimate delineation of the altitude-velocity boundaries for communications blackout.

In 1968, the Marcus Island S-band signal strength data became available for the AS-501 flight, in which an Apollo Command Module was fired into the earth's atmosphere at superorbital velocity ( $\sim$ 35,000 ft/sec). It was pertinent to the overall study, therefore, to examine the form of the plasma profile deduced on the basis of the observed AS-501 microwave signal behavior, for comparison with that determined from numerical flow field calculations.

The aim of this investigation, therefore, was to examine the effect of the Apollo afterbody plasma on the transmission of S-band (2.287 GHz) radiation by means of the microwave propagation computer programs available at CAL, and using these, to describe a plasma profile near the loss-of-signal (LOS) altitude for Apollo entry which was consistent both with the observed signal behavior from the AS-501 flight and with numerical flow field predictions. Furthermore, on the basis of a suitable derived model of the effective Apollo plasma, the possible significance of near-field effects on the overall signal attenuation was to be assessed.

## II. SIGNAL PROPAGATION CALCULATIONS

In support of other research programs involving plasma-microwave interaction studies, three computer programs have been developed at CAL for use in signal propagation calculations. The first provides for the calculation of plane-wave propagation through plasmas of arbitrarily specified number density and collision frequency.[2] By means of this program, solutions may be obtained for either TE or TM mode of propagation, for arbitrary angles of radiation incidence, and for cases wherein the plasma is bounded on both sides by free space or by free space on one side and a ground plane on the other. These options are respectively referred to herein as the free-space, $/T_{FS}/^2$, and ground plane, $/T_{GP}/^2$, transmission loss solutions.

Furthermore, since the Apollo entry environment involves propagation from an antenna in close proximity to a plasma, a second program was employed for the calculation of the admittance of an antenna radiating into a plasma, by means of which the influence of near-field and antenna impedance-mismatch effects on the overall far-field transmission loss, $/T/^2$, may be determined. This latter program assumes a rectangular waveguide antenna aperture and is based on a variational formulation due to Galejs.[3] Finally, a third computer program enables the effect of a dielectric window on the overall transmission loss to be calculated. All three programs were employed in the present investigation.

## III. EFFECTIVE MODEL OF APOLLO PLASMA BASED ON AS-501 S-BAND DATA

The signal attenuation recorded at Marcus Island during the AS-501 entry flight is shown in Fig. 1 where the S-band signal strength has been referred to the 90 dBm pre-plasma level. The figure shows the signal attenuation as a function of time during entry at a constant velocity of 35,000 ft/sec. The received signal is seen to exhibit an oscillatory behavior prior to the occurrence of a plateau, after which the signal attenuation increases monotonically to blackout. The total period of observed

change in signal level during the AS-501 entry was about 1.2 seconds, with onset of plasma-induced signal attenuation occurring at an altitude of 337,000 feet and loss-of-signal (LOS) occurring at 333,000 feet. The total altitude change over the time of interest is therefore only 4000 feet.

The oscillatory nature of the observed signal response is representative of that which occurs for a monotonic increase in the real refractive index ( $\eta_r$ from $0 \rightarrow 1$) for a low-loss ( $\nu_c/\omega << 1$) plasma slab, as a result of the cancellation and reinforcement interference of reflected waves from the front and back surfaces of the slab. The signal shown in Fig. 1 therefore indicates an underdense oscillatory behavior prior to the plateau when the plasma number density becomes critical, followed by an increasing signal attenuation with time after the plasma has become overdense to the 2.287 GHz radiation.

The initial calculations were concerned with the investigation of a simple plasma geometry to afford qualitative consistency with the observed AS-501 flight data. Accordingly, a single uniform plasma slab was considered and the plane-wave signal attenuation, $/T_{FS}/^2$, was calculated as a function of the slab electron number density, $n_e$ (or refractive index, $\eta$ ) for a range of assumed thicknesses of the slab. The critical number density for 2.287 GHz radiation is about $6.5 \times 10^{10}$ $e^-/cm^3$, whence the calculations comprised a number-density range from $10^{10}$ to $10^{11}$ for slab thicknesses from 2 to 6 freespace wavelengths ( $\lambda_o$ = 13.1 cm).

The corresponding signal attenuation is shown in Fig. 2 for selected slab thicknesses of $\ell/\lambda_o$ = 3.0 and 3.5. The attenuation has been plotted as a function of the plasma-slab refractive index and it is seen that qualitative agreement with the AS-501 data, in the occurrence of three maxima prior to the plateau at the point where the plasma becomes overdense ( $\eta_r$ = 0), indicates an effective plasma thickness of 3 $\lambda_o$ , or about 40 cm. Thicknesses for which $\ell/\lambda_o \gtrsim 3.0$ indicate either too many or too few oscillations in the underdense behavior. The correspondence for $\ell/\lambda_o$ = 3.0 is, of course, not exact as the present calculation indicates an increasing amplitude of the oscillation and attenuation levels which are higher than the flight case.

Having determined a preliminary effective slab thickness, it was then necessary to determine an appropriate estimate for the plasma collision frequency, $\nu_c$ . Calculations for normal-incidence, plane-wave signal attenuation, $/T_{FS}/^2$, were again performed, assuming a single uniform 40 cm plasma slab, for a range of collision frequencies from $10^5$ to $10^9$. The results of these calculations are summarized in Fig. 3 and show that increasing the assumed collision frequency of the plasma slab eventually destroys the oscillatory nature of the computed attenuation. Since the AS-501 flight data indicate a return to near 0 dB, relative to the 90 dBm level, following each peak in the underdense signal attenuation, these calculations indicate that the appropriate collision frequency is $\leq 10^7$. It may be noted here that the level of $10^7$ for $\nu_c$ is actually in good agreement with flow-field predictions performed for the 300,000 ft altitude case, when allowance is made for the almost order of magnitude decrease in the gas density in going from an altitude of 300,000 ft to 337,000 ft. Subsequent studies have therefore assumed a collision frequency of $\nu_c \leq 10^7$.

As far as the AS-501 flight data are concerned therefore, there is reasonable qualitative agreement as to the shape of the signal response on the basis of a single 40 cm plasma slab experiencing a temporal, monotonic increase in number density from about $4.4 \times 10^{10}$ through the critical value, with $\nu_c \leq 10^7$. However, in order to effect a better correlation with flight data, it is next necessary to investigate improvements to the above simple model, consistent with numerical predictions of the Apollo flow field.

## IV. COMPARISONS WITH PLASMA FLOW FIELD PREDICTIONS

The detailed investigations of the high-temperature air kinetics pertinent to the Apollo earth entry, which has comprised an important part of the basic research program, [1] has enabled estimates to be made of the electron number density and collision frequency distributions in the inviscid afterbody flow field. Such estimates have been obtained for the pitch-plane flow field about the Apollo vehicle at 20° angle of attack from stream-tube solutions based on pressure distributions (derived from characteristics

calculations) appropriate for various regions of the flow field. These solutions, which have incorporated the recently measured reaction rate coefficient for $NO^+$ recombination,[4] have been performed for several velocity/altitude conditions on the Apollo earth-entry trajectory.[1] The calculated flow field distribution of electron number density in the pitch plane for an illustrative trajectory point is shown in Fig. 4 in which the number density contours were determined from nonequilibrium solutions along the leeward and windward streamlines indicated in the figure. From such contour plots, the plasma profile along a desired direction of microwave propagation may be defined.

Of the many trajectory-point flow field calculations made,[1] that closest to the particular AS-501 trajectory point of interest was for a velocity of 32,000 ft/sec at an altitude of 320,000 ft. The leeward and windward number density profiles normal to the vehicle surface (the assumed direction of microwave propagation) obtained from this solution are shown in Fig. 5 and extend from the edge of the separation streamline out to the shock wave. While the indicated profiles are located at the azimuthal plane of the antennas, just downstream of the shoulder toroid, they necessarily correspond to the pitch plane of the entry attitude (Fig. 4) whereas the S-band antennas on the vehicle are actually located at about 45° with respect to the pitch plane. However, an estimated profile for the number density at the antenna location nearest to the windward side was derived from a detailed comparison of the pitch plane profiles and has been included in Fig. 5. The profile at this position has been referred to herein as that at the windward antenna location and all subsequent considerations are concerned with microwave propagation from this location.

The profiles in Fig. 5 are first seen to exhibit a gradual increase in the plasma number density with distance off the vehicle surface before undergoing a very rapid fall off in magnitude on the shock wave. This behavior indicated for the number density distribution must then be considered in any plasma model for signal propagation calculations. In the considerations that follow, the region of gradual change in number density has been referred to as region II, and the region of rapid fall off in number density as region III.

The effect of these regions on the calculated overall signal attenuation will be examined. It is further noted that since appreciable gradients in the plasma parameters occur in the calculated flow field (e.g., Fig. 4), diffusional effects, which have not been considered, would be expected to smear out such gradients in an inviscid-calculation profile and reduce the peak $n_e$ magnitudes. The influence of the size of gradients in the assumed number density profile must therefore also be examined, particularly for region II.

It can be seen from Fig. 5 that the profile for the windward antenna location, estimated on the basis of similar scaling according to the local shock layer thickness, is one which, prior to the onset of rapid fall off in the number density, is of the order of 40 cm in thickness, which is not inconsistent with the indications of the simple plasma model described previously. That is, as the shock-layer number density on earth entry increases initially from subcritical values, the signal attenuation will be determined first by the relatively uniform region II plasma with the outer, rapid fall off region III then contributing increasingly to the overall signal attenuation as its local number densities approach the critical value for 2.287 GHz radiation. In regard to overall thickness and shape, this form for the plasma profile is expected to be an adequate one for all normal-incidence propagation calculations in the interval from the onset of received S-band signal fluctuations to LOS, as the small altitude range involved ( $\sim$ 4000 ft) should result in negligible changes in flow separation behavior and shock shape.

Since the region II plasma profile indicates a gradient in the number density, it is necessary to return to the simple plasma model derived from the AS-501 flight data to determine just how steep a number density gradient can be tolerated in region II before qualitative agreement with the AS-501 S-band signal response is lost. In addition, the effect of the assumed sign of this gradient is to be examined. Accordingly, the 40 cm plasma slab was represented by 20, 2 cm thick slabs and $/T_{FS}/^2$ calculations were performed for small gradients in the overall region II profile corresponding to differences in number density between adjacent slabs of $\Delta n_e = \pm 0.2 \times 10^9$ and $\pm 0.4 \times 10^9$.

The results of these calculations are shown in Fig. 6 as a function of the region II mean-slab refractive index. The dashed profile is that for 20 identical slabs and corresponds to the 40 cm uniform-plasma slab case already discussed. It is also seen that for a profile consisting of a region II plasma only, a small gradient corresponding to a $\Delta n_e = \pm 0.2 \times 10^9$ causes essentially no change in the calculated signal attenuation compared with that for the uniform slab. However, when the gradient is increased slightly, in this case, to $\Delta n_e = -0.4 \times 10^9$, i.e., a fall off in $n_e$ with distance off the surface, the attenuation departs from close similarity with the AS-501 behavior by filling in the final trough just before the overdense plateau.

Assuming a small positive gradient of $\Delta n_e = +0.2 \times 10^9$, i.e., a gradual increase in $n_e$ with distance off the surface for the region II plasma, the region III profile was next appended in the form of an additional 20, 2 cm thick slabs whose overall number-density distribution duplicated the gradient behavior indicated in the estimated flow field profile of Fig. 5. In this case (solid curve, Fig. 6) it is seen that qualitative agreement with the AS-501 behavior is retained for a profile which is now consistent with the flow field predictions. Furthermore, it is noted that the inclusion of the outer, steep-gradient region of the shock layer plasma effects a 1-2 dB reduction in the peak attenuations resulting in an improved quantitative comparison with the AS-501 data. The correspondence is still approximate, however, as the attenuation level is still too high.

The effect of the region II plasma gradient on the overall 80 cm plasma profile (regions II and III) is further examined in Fig. 7. The solid curve is that for $\Delta n_e = +0.2 \times 10^9$, repeated from Fig. 6, and will be referred to henceforth as the basic plasma profile. The effect of an assumed $\Delta n_e = +0.4 \times 10^9$ on the overall profile, shown by the dashed curve in this figure, again shows a departure from close similarity with the AS-501 behavior in the region of the final underdense peak. Included also, is the signal attenuation calculated for the overall profile assuming a small negative gradient of $\Delta n_e = -0.2 \times 10^9$ in region II. Similarity with the flight data is also seen to be lost when the plasma is near critical and comparison of this latter behavior with that for the basic profile illustrates the fact that

the sign of even such a small gradient in the assumed profile for region II has a significant effect on the calculated underdense signal attenuation. Finally, since the maximum gradient investigated for region II ( $\Delta n_e = 0.4 \times 10^9$) represents, for example, an increase in number density from only 6.00 to 6.76 x $10^{10}$ over a distance of 40 cm, the above results indicate strongly that this important region of the Apollo earth-entry plasma is one of essentially constant number density.

## V. ADDITIONAL CONSIDERATIONS APPROPRIATE TO THE APOLLO ENVIRONMENT

### 5.1 Indication of the Effect of Dielectric Material Over the Antenna Aperture Plane

The aperture ground plane on the Apollo Command Module is covered by an ablative dielectric material, about 1-inch thick, having a nominal dielectric constant, $\varepsilon'/\varepsilon_o = 2.0$. Calculations were therefore made for the effect of such a dielectric slab immediately adjacent to the basic plasma profile. While solutions were obtained both for the lossless case and for an assumed loss tangent, $\varepsilon''/\varepsilon' = 0.01$, no significant difference was found between these two cases and the computed signal attenuation, $/T_{FS}/^2$, is shown in Fig. 8 (curve B). The attenuation for the basic plasma profile alone has also been included for comparison (curve A). Qualitative agreement with the AS-501 signal response is seen to be retained with the net effect of the dielectric slab being to increase the overall signal attenuation by about 2 dB, resulting now in an increased departure from the actual measured attenuations. It is noted, however, that on the basis of these simple-model plane-wave calculations, this discrepancy cannot be reduced simply by adjustment of the plasma thickness since such adjustment would also reduce the effective $\ell/\lambda_o$ of the plasma and yield an underdense signal behavior contrary to the AS-501 data (Fig. 2). It will be necessary, therefore, to examine the influence of antenna impedance mismatch and near-field effects upon the calculated far-field transmission loss to effect any further possible correlation between the flight data and theoretical predictions.

It will be shown below that the inclusion of these effects requires the solution for the ground-plane transmission loss, $/T_{GP}/^2$, which solution is readily obtained by means of the computer program for plane-wave propagation discussed at the outset. The form of this solution for the basic plasma profile is shown in Fig. 9. The ground-plane transmission loss calculated for a single uniform 40 cm plasma slab has also been included (dashed curve) for comparison. The signal attenuation assuming the plasma to be bounded on one side by a conducting ground plane is also seen to exhibit the oscillatory behavior characteristic of the flight case although the indicated peak attenuations are considerably higher than for the free-space bounded profile.

## 5.2 Effect of a Region of Separated Flow

For signal propagation from the Apollo vehicle, the transition from dielectric to dissipative medium is not abrupt since a region of separated flow exists between the antenna aperture plane and the high-number-density inviscid hypersonic plasma. In order, therefore, to improve the model for the Apollo afterbody plasma, it is necessary to take account of the fact that the plasma itself is not immediately adjacent to the vehicle surface. Within the current capabilities for flow field calculation, however, the location of the separation streamline at the windward antenna position cannot be defined precisely, although a consideration of the pitch-plane estimates for this region indicates a thickness of the order of 4 cm over the antenna. However, since the actual location of the plasma with respect to the aperture plane will affect the overall signal attenuation, it is necessary to investigate the effect of the assumed thickness of the separated flow region on the attenuation calculations.

The separated flow region, designated region I, is expected to be one of comparatively low number density, exhibiting a rapid fall off in electron concentration towards the cold-wall surface because of the absence of appreciable heating effects at these altitudes ($\sim$ 335,000 ft), and hence the absence of significant ablative material contributions to the number density. No estimate of the plasma properties in this region has been included here. It is noted that Rae[5] has described a semi-empirical method for the calculation of equilibrium-flow profiles consistent with enthalpy and velocity profiles

through a region of separated flow, derived to match measured heat-transfer data and separation streamline conditions. However, the method is applicable to the axisymmetric case only and assumes no normal pressure gradient. Its application to the present 20° angle of attack geometry is therefore not strictly justificable and such calculations for the region I plasma have not been included lest unjustified credence be given to number-density magnitudes so derived. Instead, region I has been represented as a low number density, collision-frequency slab ( $n_e = \nu_c = 10^6$), more for purposes of avoiding possible computational difficulties in the antenna admittance calculations than as an assumed suitable representation of the plasma conditions in this region.

In the remaining calculations, attention has been focused only on a specific, representative point in the "temporal" profile of the signal attenuation; that for which the plasma conditions correspond to the final peak in the underdense attenuation. At this point, which is indicated in Fig. 8, the mean number density is $\bar{n}_e = 6.2 \times 10^{10}$.

The effect of displacing the plasma off the vehicle surface is shown in Fig. 10. As before, the basic profile shape has been assumed and the signal attenuation is presented as a function of the thickness of the region I slab. Both the $/T_{FS}/^2$ (dashed curves) and $/T_{GP}/^2$ (solid curves) solutions are shown for cases with and without the low-loss dielectric covering the aperture plane. The results assuming only a single uniform 40 cm plasma slab have again been included for comparison. With no dielectric present, the free-space transmission loss, $/T_{FS}/^2$, is, of course, constant and as could be seen earlier (Fig. 5, $\eta = 0.22$) the attenuation assuming the basic profile is reduced from that for the single 40 cm slab by about 1 dB. When the plasma is immediately adjacent to the surface, the ground-plane transmission loss is seen to be about twice the free-space loss, but then to decrease with an increase in the separation region thickness. The $/T_{GP}/^2$ solution is actually oscillatory although only about half the period has been shown. With the low-loss dielectric slab assumed to cover the aperture plane, both the $/T_{FS}/^2$ and $/T_{GP}/^2$ solutions exhibit an oscillatory behavior of similar period, with increase in the separated-region thickness. The ground-plane solution in this case, however, is seen to be inverted over that in the absence

of the ablative dielectric. While the above $/T_{GP}/^2$ solutions appear to indicate a net gain in signal strength for a certain thickness range of the separated-flow region, this is actually artificial. As mentioned earlier, the purpose here was merely to illustrate the form exhibited by the $/T_{GP}/^2$ solutions. By itself, $/T_{GP}/^2$ is not representative of actual attenuation effects. It will be shown below that the $/T_{GP}/^2$ solution enters into the calculation of the actual far-field transmission loss in which, however, its magnitude is attenuated by a factor involving the antenna admittances.

## VI. CONSIDERATION OF ANTENNA-ADMITTANCE VARIATION EFFECTS ON THE TRANSMISSION LOSS

At this point, the effects of antenna-admittance variations on the far-field signal attenuation will be considered. Previous analytical and experimental studies at CAL of microwave propagation through aerodynamically-generated hypersonic plasmas from aperture antennas terminating on a conducting ground plane have included the consideration of antenna impedance mismatch and near-field effects in calculating the far-field signal attenuation. It may be shown[6] that the overall transmission loss in the presence of a plasma, $/T/^2$, for an aperture antenna in a conducting plane excited from a matched source, which takes account of these effects, can be written as

$$|T|^2 = |T_{GP}|^2 \frac{Re\, Y_o}{Re\, Y_p} \left( \frac{1 - |\Gamma_p|^2}{1 - |\Gamma_o|^2} \right) \qquad (1)$$

In this expression, $/T_{GP}/^2$ is the plane-wave ground plane signal attenuation discussed previously, $Re\, Y_p$ and $Re\, Y_o$ are, respectively, the real parts of the antenna admittance (i.e. antenna conductance) with and without the plasma, and $\Gamma_p$, $\Gamma_o$ are, respectively, the voltage reflection coefficients at the antenna with and without the plasma. The first two terms on the right side of Eq. (1) represent the near-field effects and relate to the antenna efficiency, or ratio of the power in the far field to the total power radiated. The last term is the relative mismatch loss due to antenna impedance variations. The above expression for the antennuation, referred to

free space, may be rewritten more conveniently as

$$|T|^2 = |T_{GP}|^2 \left| \frac{Y_o + Y_G}{Y_p + Y_G} \right|^2 \qquad (2)$$

where $Y_o$ is the complex free-space antenna admittance, $Y_G$ is the waveguide admittance (generator assumed matched to guide) = 1.0 for an open, unloaded waveguide, and $Y_p$ is the complex aperture admittance in the presence of the plasma. For given waveguide dimensions, $Y_o$ is obtained from published charts (present case: $Y_o = 0.925 + j0.38$) and $Y_p$ is determined from an admittance calculation. Equation (2) shows that the far-field signal attenuation, including near-field and mismatch effects, is given by the ground-plane transmission loss, attenuated by the factor

$$10 \log \left| \frac{Y_o + Y_G}{Y_p + Y_G} \right|^2 dB$$

It is important to note here that the present calculations for the antenna admittance, $Y_p$, were obtained by means of a computer program employing a variational formulation due to Galejs.[3] This formulation, however, assumes a rectangular waveguide terminating in a ground plane, with aperture excitation in the principal ($TE_{10}$) mode. The Apollo vehicle S-band antenna on the other hand is a circular waveguide operating in the $TE_{11}$ mode. The present calculations, which have assumed a rectangular waveguide of a size consistent with dominant mode operation at a frequency of 2.287 GHz, must therefore be taken as indicative of a trend.

As before, a single illustrative plasma profile has been considered, corresponding to an altitude for which the mean region II number density is $\bar{n}_e = 6.2 \times 10^{10}$, representing the final peak in the underdense attenuation response (Fig. 8). Owing to the demonstrated sensitivity of the previous $/T_{FS}/^2$ and $/T_{GP}/^2$ attenuation calculations to slight changes in the assumed shape and extent of the plasma profile, the sensitivity of the admittance calculations for $Y_p$ was also examined for similar changes in the number-density distribution. These latter calculations, however, were found to be

reasonably insensitive to such profile geometry changes as may be seen in the accompanying table. Effects are seen to be largest on the conductance, the actual magnitude of which, however, is very small in these cases, whereas the susceptance is reasonably insensitive to variations in $Y_p$ are seen to have a negligible effect on the magnitude of the $\left|\frac{Y_o + Y_a}{Y_p + Y_a}\right|^2$ term. These results appear consistent with the empirical criterion indicated by Swift[7]

| Plasma Model | Antenna Admittance $Y_p$ | $\left\|\frac{Y_o + Y_a}{Y_p + Y_a}\right\|^2$ |
|---|---|---|
| 20 Slab II and III ( $\Delta n_{e_E} = +0.2 \times 10^9$) | 0.01635 - j.2666 | +5.43 dB |
| 20 Slab II only ( $\Delta n_{e_E} = +0.2 \times 10^9$) | 0.027 - j.2666 | +5.34 |
| 40 cm Uniform Slab only | 0.01315 - j.3018 | +5.36 |
| 20 cm Uniform Slab only | 0.0082 - j.310 | +5.39 |

viz, $e^{-2\alpha_p l} > 0.1$, where $\alpha_p$ is the attenuation constant and $l$ the plasma thickness, to indicate a situation under which the admittance is independent of the plasma thickness. In the above calculations, $e^{-2\alpha_p l} \sim 1$. Since the computing time for the antenna admittance calculations is dependent on the number of plasma slabs, the above results therefore allowed this time to be minimized by representing the plasma as a single uniform 40 cm thick slab for purposes of calculating $Y_p$ only. It is reiterated, however, that the calculated far-field signal attenuation, $/T/^2$ is sensitive to the profile variations indicated in the above table, this sensitivity arising solely because of their effect on the magnitude of $/T_{GP}/^2$. In the calculations for $/T/^2$, therefore, the value of $/T_{GP}/^2$ appropriate to the basic plasma profile was employed in the Eq. (2) calculations.

The calculated far-field signal attenuation for the basic plasma profile is shown in Fig. 11 as a function of the thickness of the separated flow region. It is seen that when the plasma is immediately adjacent to the ground plane, the far-field loss is essentially equal to the plane-wave free-space loss, $/T_{FS}/^2$. However, as the assumed plasma profile is moved away from the vehicle surface, the inclusion of near-field and impedance-mismatch

effects results in a reduction of the far-field transmission loss from the free-space plane-wave loss.

The corresponding peak attenuation exhibited in the AS-501 flight data was about 2.5 dB, which value is obtained in the present calculations when the plasma is about 2.5 cm off the surface. The above investigation indicates, therefore, that the inclusion of near-field effects and antenna impedance variations is necessary to afford quantitative agreement between the AS-501 signal attenuation data and calculations based on a plasma geometry consistent with the flow field predictions.

Unfortunately, it was not possible with the present CAL computer program to calculate the antenna admittance, $Y_a$, for the case with the low-loss dielectric slab over the aperture plane. Such calculations exhibited an untenable variation in the antenna susceptance, although the conductance appeared to be fairly well behaved. This behavior probably represents the appearance of surface-wave effects in which energy is confined within the dielectric slab as surface waves. In certain regions of the calculation for a low-loss dielectric, the integrands in the admittance expression[3] can become very large and the present program has not been modified to account for surface-wave pole contributions to the admittance in such cases. It is possible that this problem could have been circumvented to some extent in the present case by assuming an artificially large loss tangent for the dielectric material. Suitable computational techniques are available, however, for such calculations. Croswell et al.[8] for example, have investigated the effect of finite ground-plane size on the calculated admittance of a rectangular waveguide radiating into a low-loss dielectric slab ($\varepsilon'/\varepsilon_0 = 3.76$) in which the contribution of the surface-wave conductance to the total conductance was included. Similarly, Bailey and Swift[9] have described aperture admittance calculations for a circular waveguide operating in the $TE_{11}$ mode, radiating into the same dielectric slabs employed by Croswell,[8] in which surface-wave conductance contributions were also included. Parenthetically, these latter investigations indicated that in the case of the circular waveguide, the energy trapped inside the dielectric was only about half that confined within the same dielectric for the rectangular waveguide case.

## VII. INDICATION OF THE EFFECT OF AN ANTENNA WINDOW ON THE TRANSMISSION LOSS

The investigations of signal attenuation considered thus far have assumed an unloaded (open) waveguide whereas the Apollo vehicle S-band antenna necessarily has a dielectric window (plug) in the guide. Notwithstanding the differences between the assumed and actual waveguide geometries, additional calculations of the far-field signal attenuation were therefore performed for the case of a dielectrically-loaded rectangular waveguide radiating into the basic plasma profile ( $\bar{n}_{e_x} = 6.2 \times 10^{10}$). These calculations were again performed for the purpose of indicating the behavioral trend and since the means for such computation was available, their inclusion is within the stated aim of the present investigation.

The particular dielectric window employed on the AS-501 vehicle had a dielectric constant $\varepsilon'/\varepsilon_o = 3.35$ (fused quartz) for which a loss tangent $\varepsilon''/\varepsilon' = 10^{-4}$ at S-band, was assumed. The calculations considered a range of plug thicknesses from 0.1 inch to 2.0 inch and the resultant far-field signal attenuation is shown in Fig. 12 as a function of window thickness, for several assumed thicknesses of the separated-flow region. For the reasons stated earlier, the effect of an ablative dielectric over the aperture ground plane could not be included in these calculations. The results show that for a given distance of the plasma off the aperture plane, the transmission loss undergoes an oscillation with increasing window thickness, with the largest oscillation amplitude occurring when the plasma is immediately adjacent to the ground plane (d = 0). As the plasma is moved away from the ground plane, the oscillations in overall transmission loss are reduced slightly in amplitude with the maximum transmission loss occurring at progressively smaller window thickness. The "wavelength" of the oscillation in transmission loss corresponds to a change in window thickness of about 1.5 ins., or about a half-wavelength in the loaded guide, $\lambda_{G,diel}/2$ where

$$\lambda_{G,diel} = \frac{\lambda_o}{\sqrt{\varepsilon'/\varepsilon_o - \left(\frac{\lambda_o}{2a}\right)^2}} = 7.6 \text{ cm} = 3 \text{ in.}$$

The above information is also presented in a slightly different form in Fig. 13 in which the far-field transmission loss is shown as a function of the thickness of the separated-flow region for several thicknesses of the antenna window. The case for the open waveguide (t=0) discussed previously (Fig. 11) has also been included for comparison. The profiles for the selected window thicknesses shown in this figure bracket the maximum variations in the computed far-field transmission loss for any window thickness. The presence of a window of dielectric constant 3.35 in the guide is seen to increase the far-field signal attenuation over that for the open waveguide although the attenuation for the loaded guide decreases more rapidly as the plasma is moved off the surface. For the range of window thicknesses assumed, quantitative agreement with the observed AS-501 signal attenuation indicates a separated-flow region thickness of from 2 to 3 cm, as for the open guide case. It should be mentioned that the above antenna admittance calculations for the dielectrically-loaded waveguide have assumed that a dominant-mode aperture-field distribution is adequate and that the dielectric window does not become a resonant cavity for a higher mode for certain window thicknesses at the 2.287 GHz frequency.[10]

## VIII. EFFECT OF RADIATION PROPAGATION ANGLE

Since the observed oscillatory response shown by subcritical levels of the number density has been shown to be quite sensitive to the thickness and gradient of the region II plasma, it was considered informative to investigate, within the limitations of plane-wave electromagnetic calculations, the effect of angle of propagation through the plasma on the transmitted signal behavior. Signal attenuation calculations were therefore performed for propagation paths through the plasma (regions II and III) at angles up to 20° off the normal to the antenna aperture. While the assumed plasma profile comprised both regions II and III, the region II plasma was simply represented by a single uniform 40 cm plasma slab. For purposes of illustrating the effect of angle of radiation incidence, however, this profile should be quite suitable. Furthermore, for qualitative assessment, only the free-space transmission loss, $/T_{FS}/^2$, was calculated. The effect of angle of incidence

on the assumed planar plasma geometry is shown in Fig. 14 where it is seen that similarity with the observed AS-501 data exists only for propagation paths within about 10° of the aperture normal. It is noted, however, that the effects of local curvature of the ground plane, the dielectric covering and of the plasma itself have not been considered here, whence correlation with the observed signal response may not necessarily be restricted to the small viewing angles implied by the above calculations.

## IX. SUMMARY

A simple investigation has been made of S-band signal transmission through an Apollo earth-entry plasma in which recourse was made to signal attenuation data recorded from the AS-501 flight. Within the capabilities of the available computer programs at CAL, a plasma profile near the LOS altitude for the AS-501 entry has been described which is consistent both with the observed signal behavior and with the Apollo flow field predictions. The investigation has further indicated that plane-wave analyses alone are inadequate and that antenna near-field and impedance mismatch effects must be included to afford a quantitative comparison with the AS-501 data.

In the absence of a low-loss dielectric material over the ground plane, but including the effects of a dielectrically-loaded (rectangular) aperture antenna, the results of transmission-loss calculations indicate a separated flow region thickness of from 2 to 3 cm, in reasonable accord with the 4 cm thickness estimated from the flow-field solutions. Furthermore, in the assumed absence of ground plane and plasma curvature effects, such calculations in the AS-501 case indicate S-band signal reception corresponding to a propagation path close ( $\leq 10°$) to the transmitting aperture normal.

## REFERENCES


1. Dunn, M.G., Final Report Project Apollo.

2. Bein, G.P., Plane Wave Propagation at Arbitrary Angles of Incidence in Inhomogeneous, Lossy Plasmas and Prediction of Antenna Radiation Patterns, CAL Rept. ER/RIS-8, Jan. 1966.

3. Galejs, J., Admittance of a Rectangular Waveguide Radiating into Stratified Plasma, IEEE AP-13, 64 (1965).

4. Dunn, M.G., Lordi, J.A., Measurement of $NO^+ + e^-$ Dissociative Recombination in Expanding Air Flows, CAL Rept. AI-2187-A-10, Sept. 1968.

5. Rae, W.J., A Method for Estimating Separated-Flow Profiles Over an Asymmetric Afterbody, CAL Rept. AI-2187-A-7, Oct. 1967.

6. Veron, H., Andre, S.N., EM Wave Propagation, Antenna Admittance and Antenna Coupling Effects in a Plasma Environment, CAL Rept. VI-2052-E-1, April 1967.

7. Swift, C.T., Input Admittance of a Rectangular Waveguide-Fed Aperture Antenna Radiating into an Inhomogeneous Lossy Dielectric Slab, NASA TN D-4197, Oct. 1967.

8. Croswell, W.F., Rudduck, R.C. and Hatcher, D.M., The Admittance of a Rectangular Waveguide Radiating into a Dielectric Slab, IEEE Trans. Antennas and Propagation, Vol. AP-15, 627, Sept. 1967.

9. Bailey, M.C. and Swift, C.T., Input Admittance of a Circular Waveguide Aperture Covered by a Dielectric Slab, IEEE Trans. Antennas and Propagation, Vol. AP-16, 386, July 1968.

10. Swift, C.T. and Hatcher, D.M., The Input Admittance of a Rectangular Aperture Antenna Loaded with a Dielectric Plug, NASA TN D-4430, April 1968.

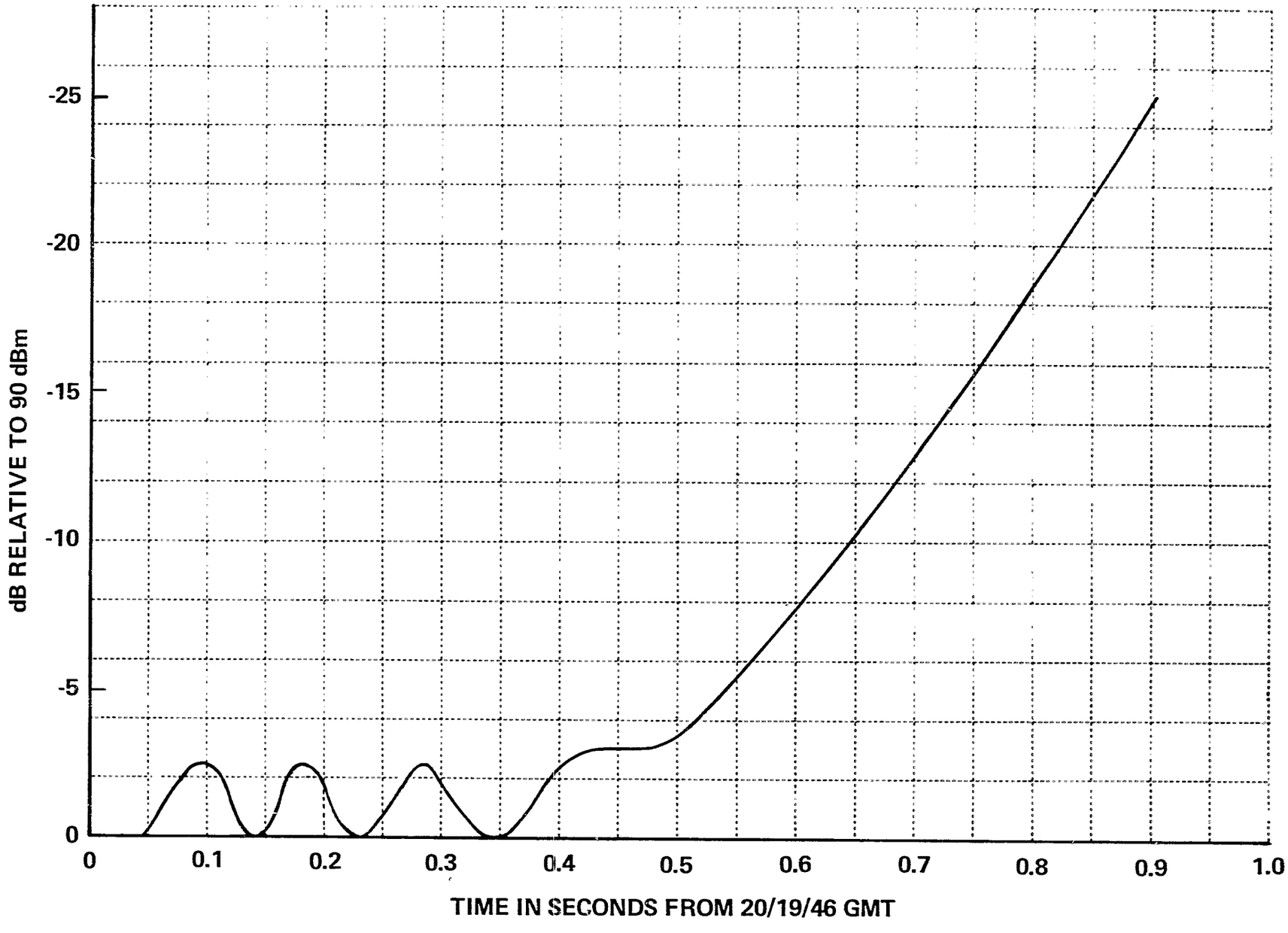


Figure 1 2.287 GHz SIGNAL ATTENUATION RECORDED FROM AS 501 FLIGHT

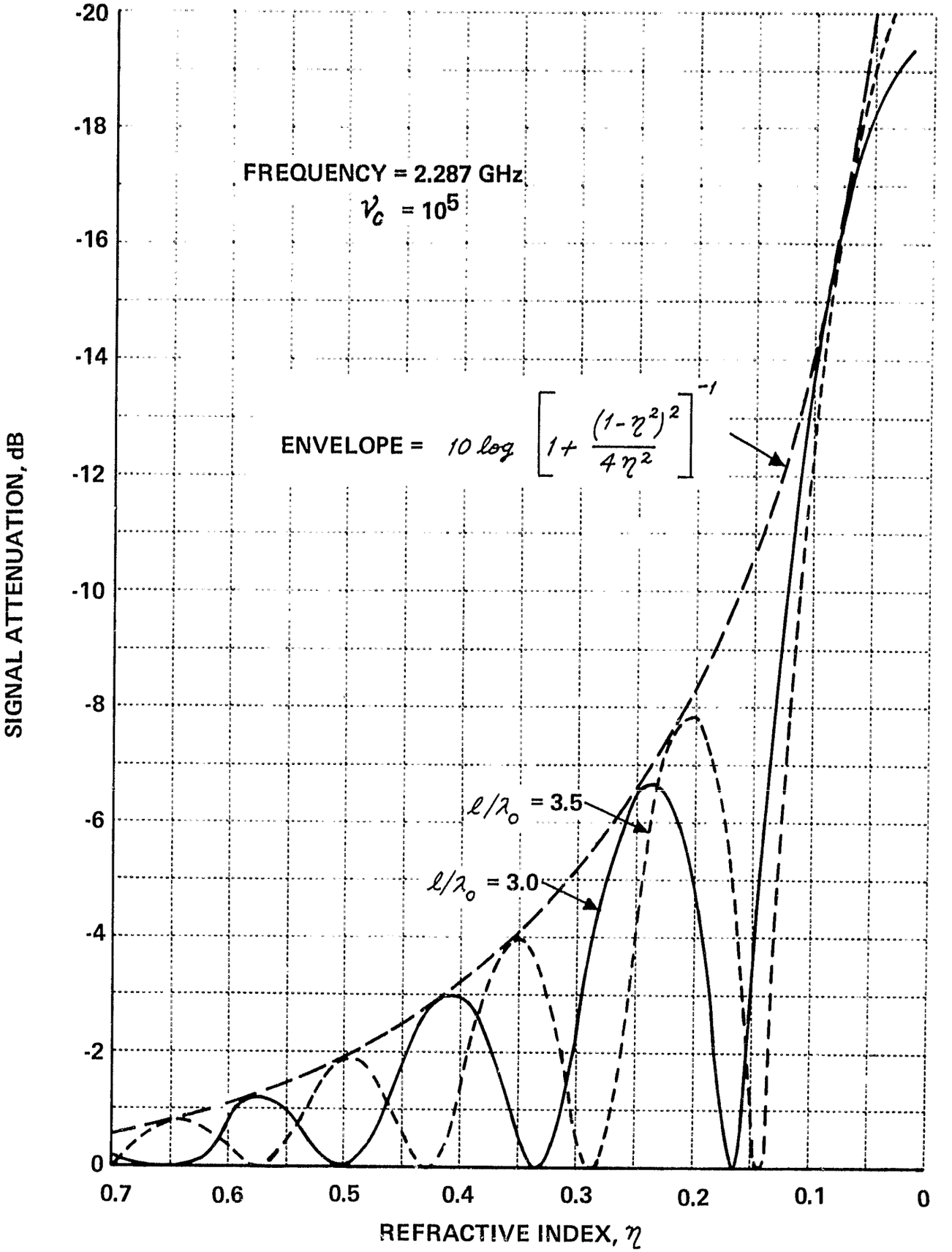


**Figure 2** EFFECT OF PLASMA THICKNESS ON UNDERDENSE SIGNAL ATTENUATION BEHAVIOR

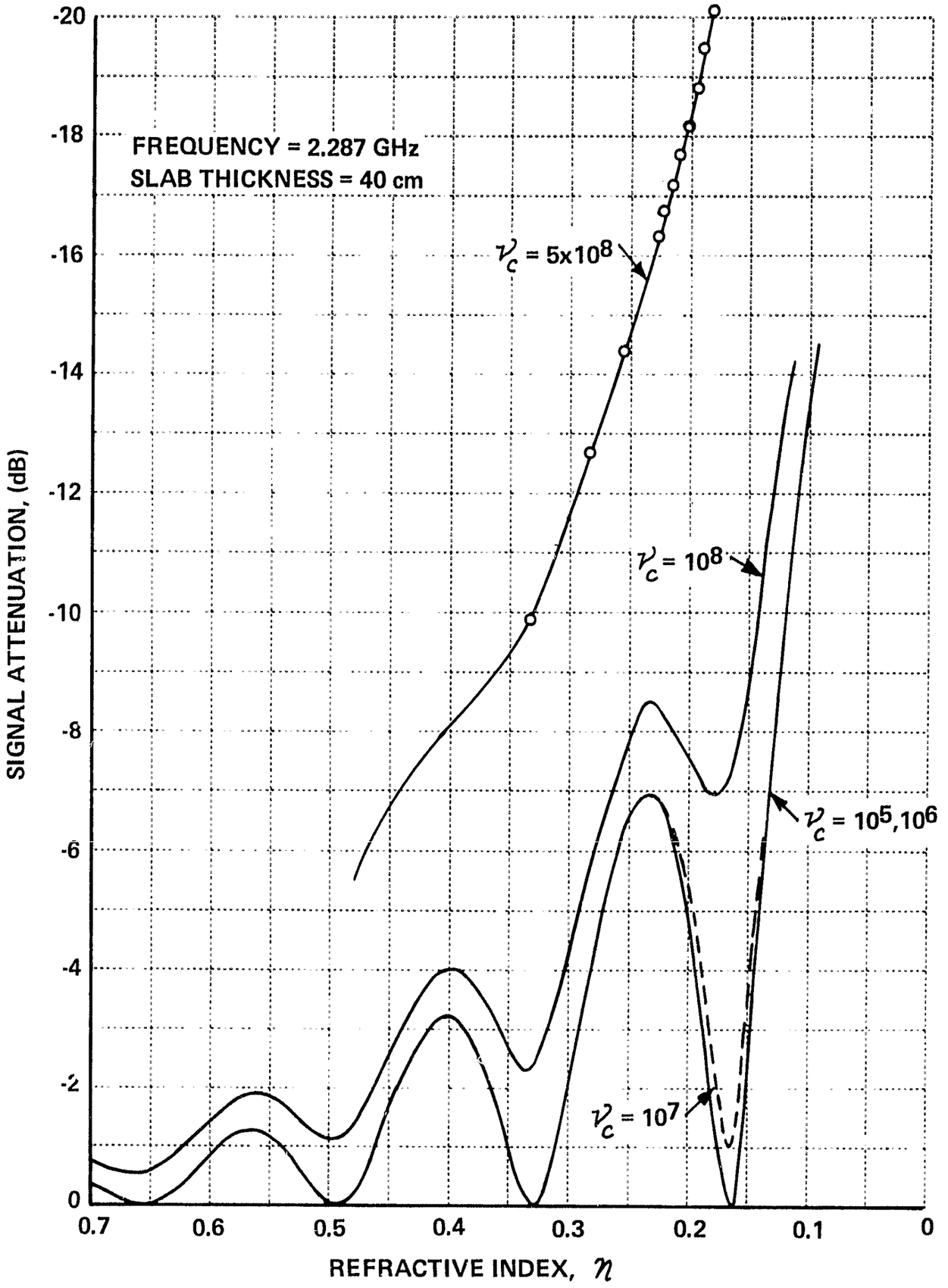


Figure 3 EFFECT OF COLLISION FREQUENCY ON SIGNAL ATTENUATION

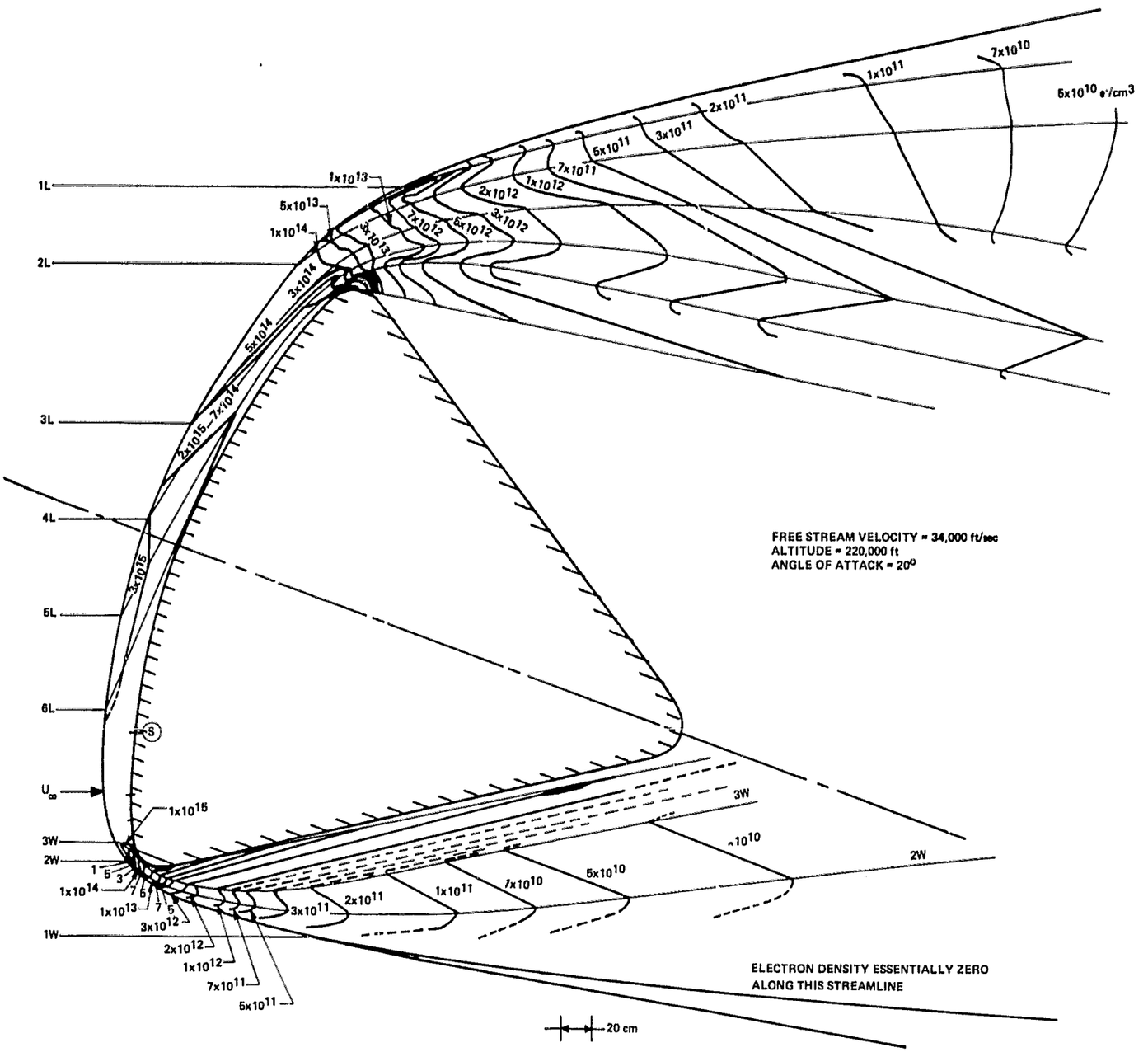


**Figure 4 ELECTRON-DENSITY DISTRIBUTION**

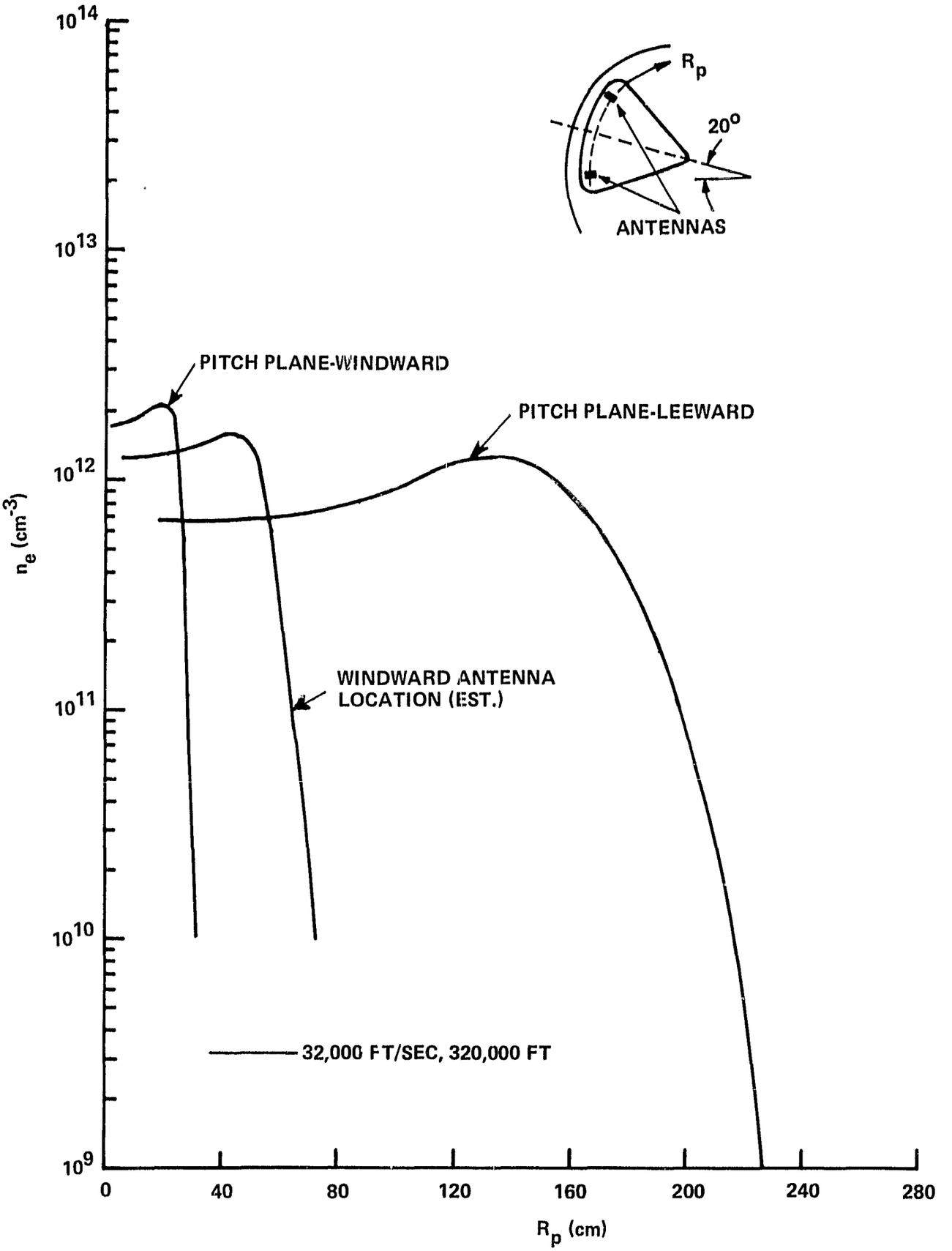


Figure 5 NUMBER DENSITY PROFILES NORMAL TO BODY SURFACE

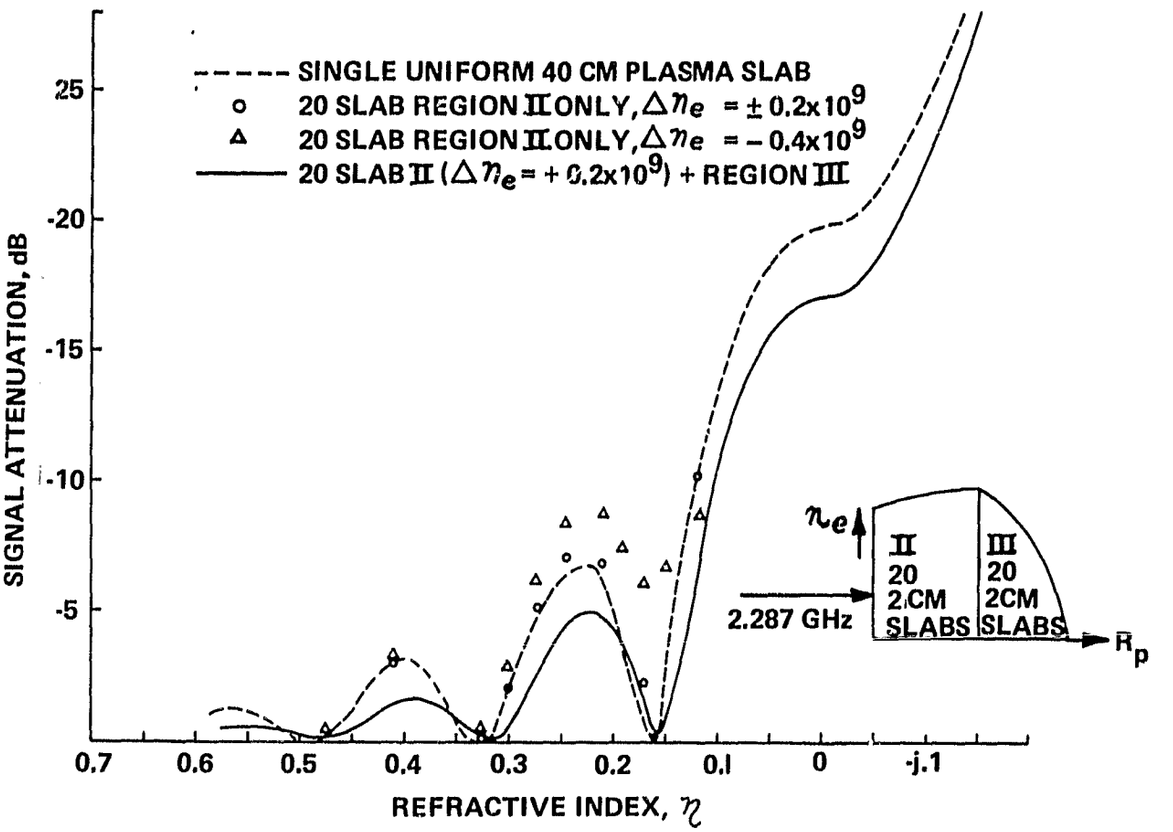


Figure 6 EFFECTS OF SMALL GRADIENT IN REGION II ELECTRON NUMBER DENSITY

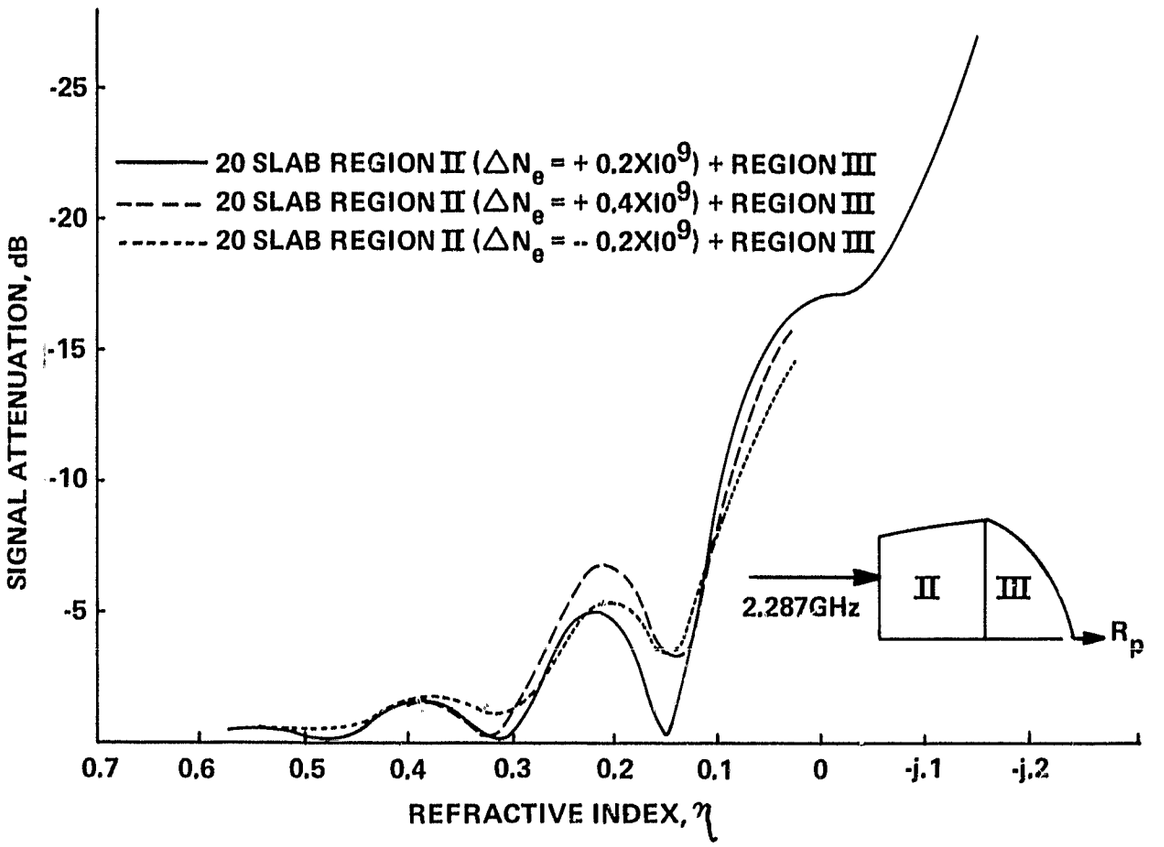


Figure 7 EFFECT OF SMALL GRADIENT IN REGION II ELECTRON NUMBER DENSITY

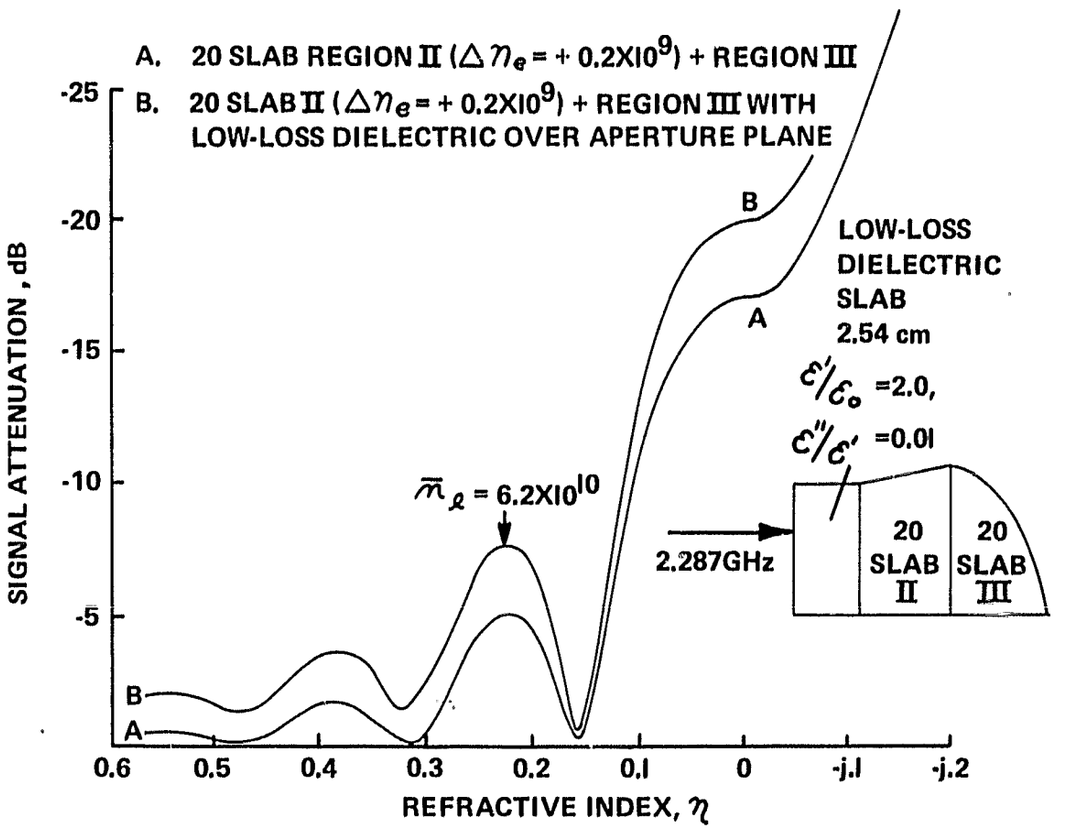


**Figure 8** EFFECT OF DIELECTRIC SLAB OVER GROUND PLANE ON TRANSMISSION LOSS

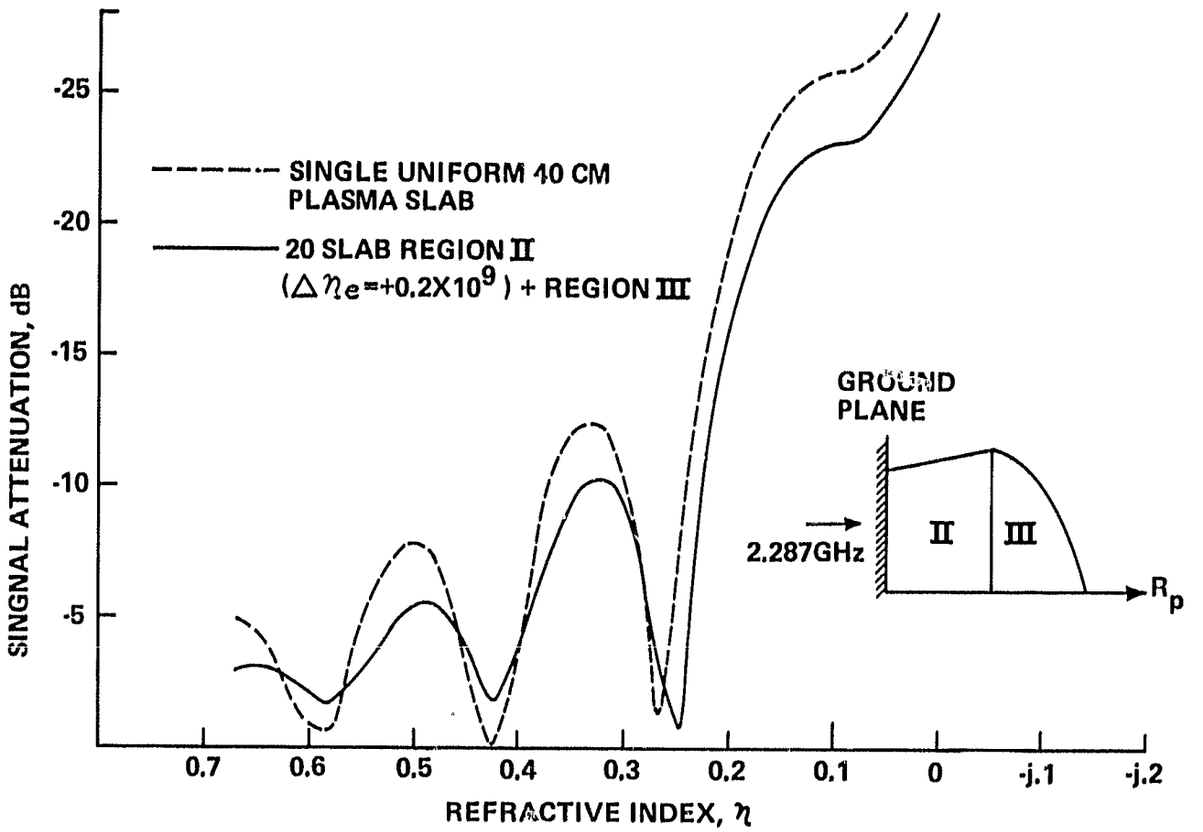


Figure 9 GROUND PLANE TRANSMISSION LOSS

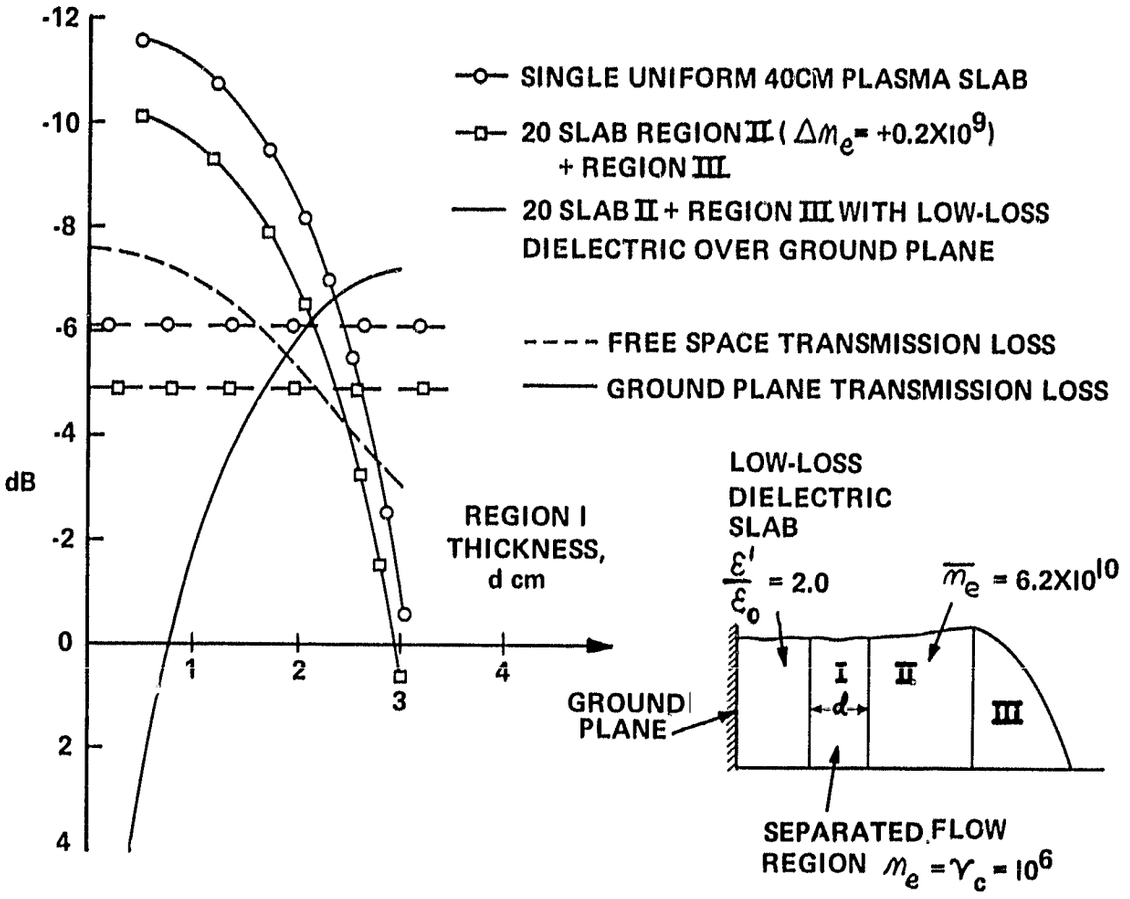


Figure 10 TRANSMISSION LOSS AS FUNCTION OF DISTANCE OF PLASMA OFF GROUND PLANE

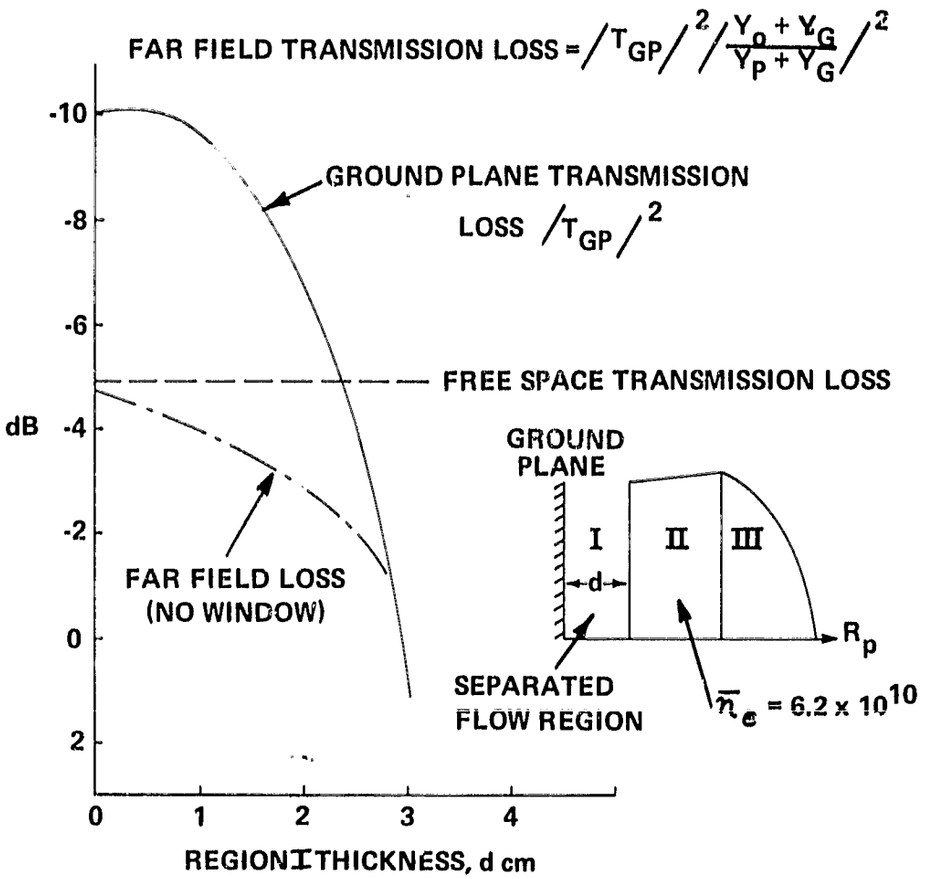


Figure 11 FAR FIELD TRANSMISSION LOSS AS FUNCTION OF DISTANCE OF PLASMA OFF GROUND PLANE

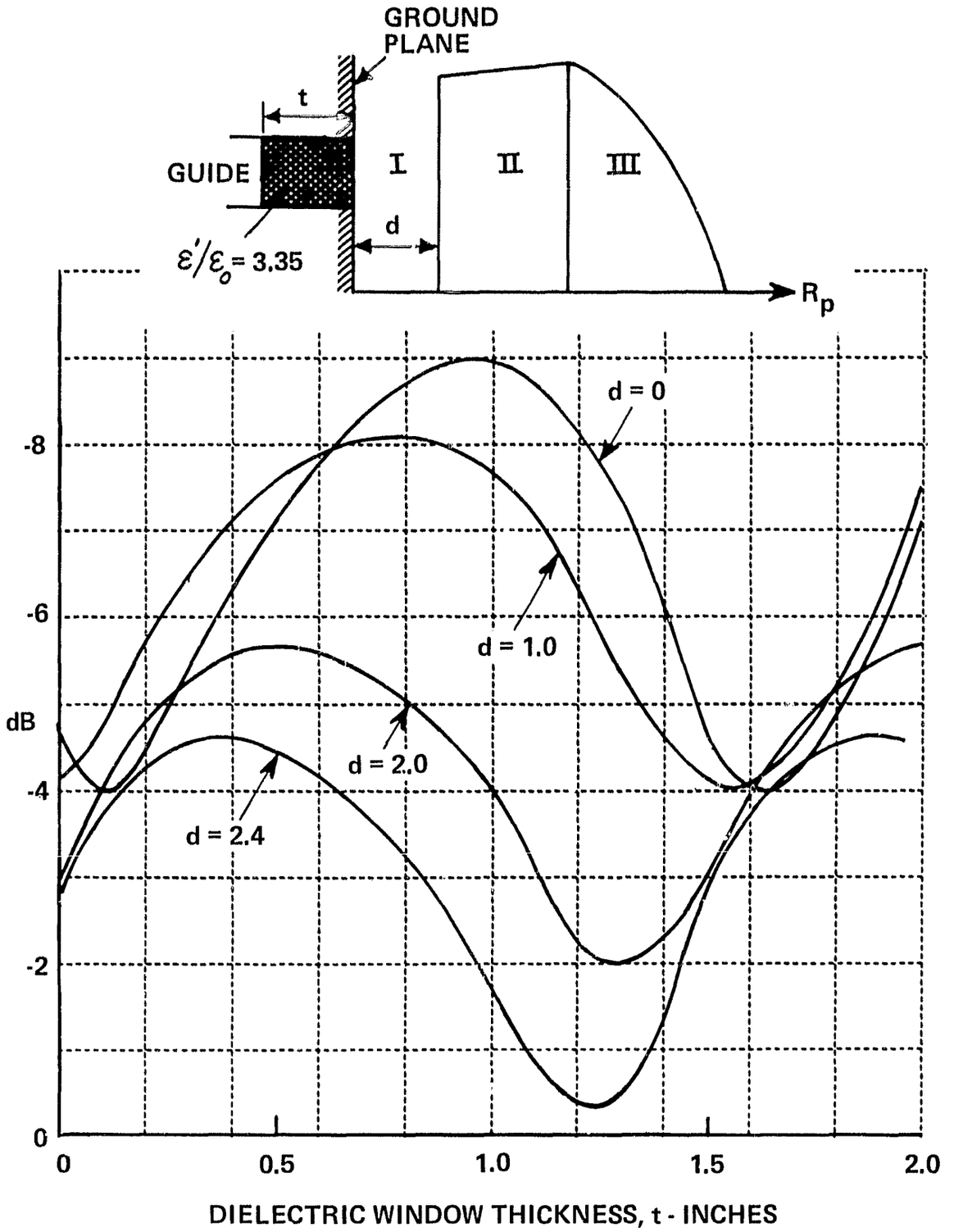


Figure 12 FAR FIELD SIGNAL ATTENUATION AS A FUNCTION OF ANTENNA WINDOW THICKNESS

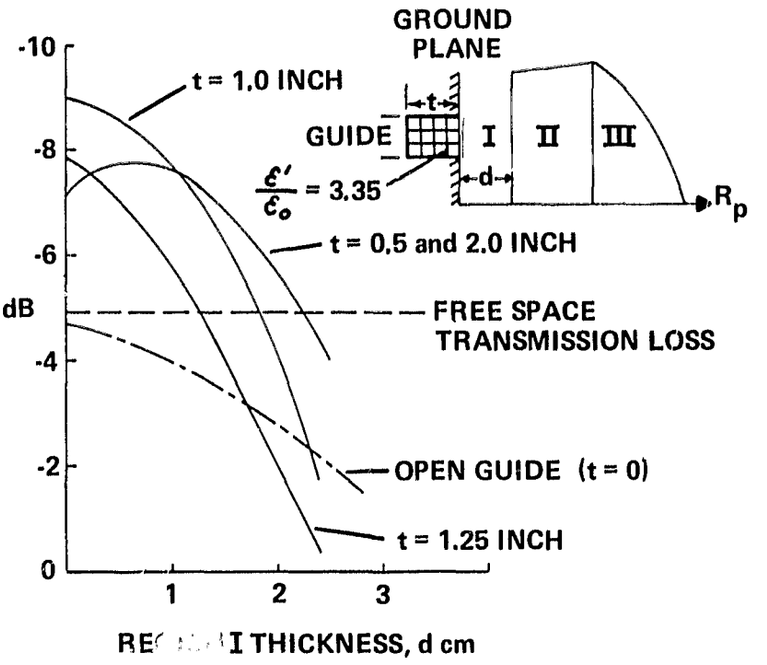


Figure 13 EFFECT OF ANTENNA WINDOW THICKNESS ON FAR-FIELD TRANSMISSION LOSS

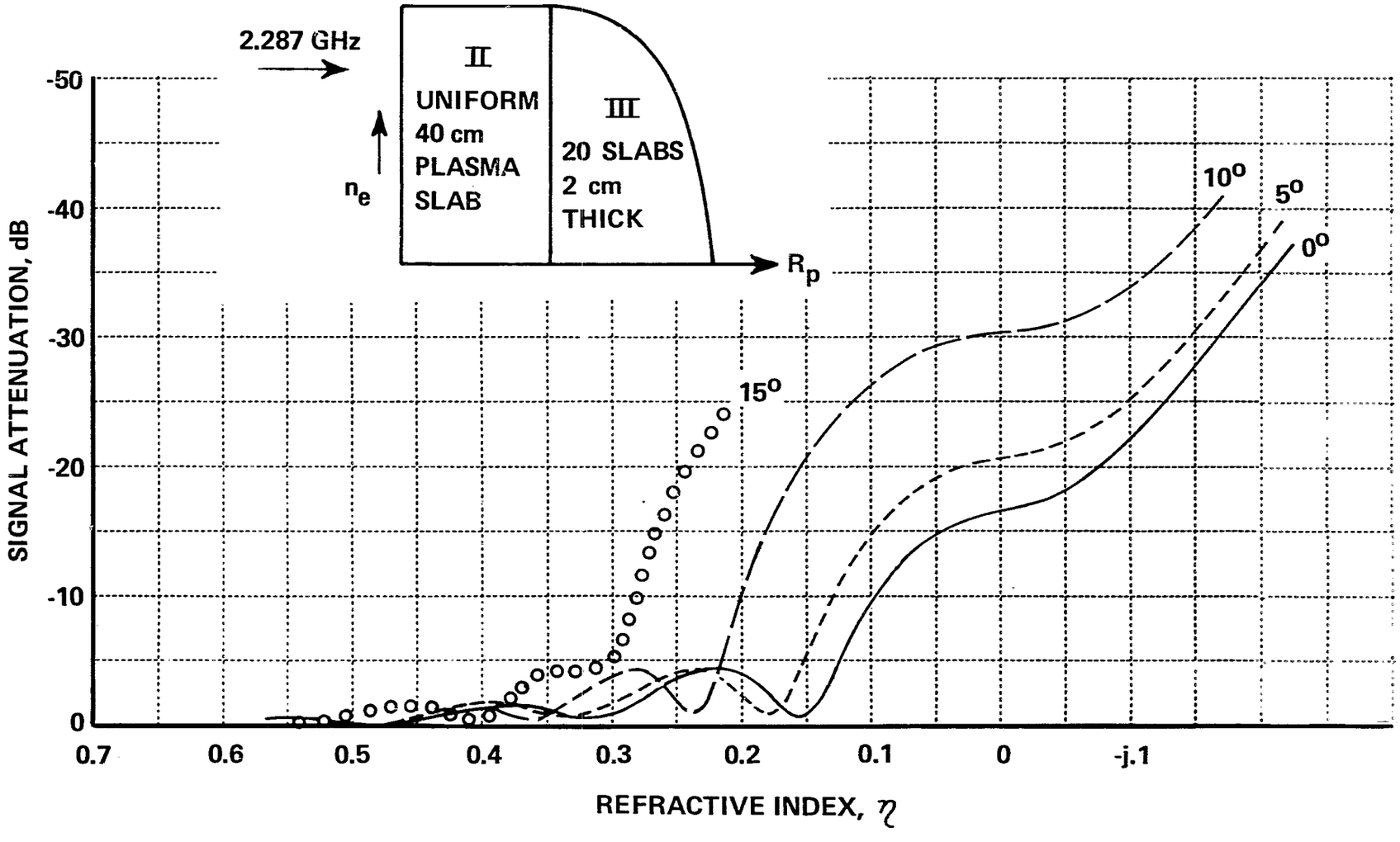


Figure 14 PLANE-WAVE TRANSMISSION LOSS AS FUNCTION OF RADIATION INCIDENCE ANGLE